Structural Engineering and Mechanics, Vol. 8, No. 6 (1999) 623-637
DOI: http://dx.doi.org/10.12989/sem.1999.8.6.623

Assumed strain quadrilateral C^0 laminated plate element based on third-order shear deformation theory

G. Shi†, K.Y. Lam‡ and T.E. Tay‡†

Institute of High Performance Computing, National University of Singapore, Singapore 119260

J.N. Reddy‡

Department of Mechanical Engineering, Texas A & M University, TX, U.S.A.

Abstract. This paper presents a four-noded quadrilateral C^0 strain plate element for the analysis of thick laminated composite plates. The element formulation is based on: 1) the third-order shear deformation theory; 2) assumed strain element formulation; and 3) interrelated edge displacements and rotations along element boundaries. Unlike the existing displacement-type composite plate elements based on the third-order theory, which rely on the C^1-continuity formulation, the present plate element is of C^0-continuity, and its element stiffness matrix is evaluated explicitly. Because of the third-order expansion of the in-plane displacements through the thickness, the resulting theory and hence elements do not need shear correction factors. The explicit element stiffness matrix makes the present element more computationally efficient than the composite plate elements using numerical integration for the analysis of thick layered composite plates.

Key words: laminated composite plates; Reddy-Levinson third-order plate theory; plate element; assumed strain FE formulation.

1. Introduction

Because of the high strength-to-weight ratio in the preferred directions, laminated composite plates are widely used in various engineering applications. On the other hand, laminated composite plates made from unidirectional fibre-reinforced laminae have low transverse shear stiffness. This means that transverse shear deformations in composite plates play a more significant role both in deflections and failure modes than they are in isotropic plates. Therefore, many shear deformation theories, including the first-order and higher-order shear deformation theories, have been proposed for analysing laminated composite plates (see e.g., Reddy 1997). In the first-order shear deformation theories, shear correction factors are needed. Unlike in the case

† Ph.D.
‡ Professor
‡† Associate Professor

of the isotropic plates where the shear correction factor is a constant, the shear correction factors in composite plates depend on lamina orientations and stacking sequence. However, no shear correction factors are needed in higher-order theories of composite plates. A comparative study (Rohwer 1991) showed that the simple third-order shear deformation theory (STSDT) of Reddy-Levinson (Reddy 1984, Levinson 1980) is one of the best higher-order theories. This is because this theory uses fewer field variables but gives good results not only for deflections but also for in-plane displacements and stresses across the plate thickness.

The displacement-based finite element formulation for the higher-order theories is more complicated than that for the first-order theories. This is because more nodal degrees of freedom are needed in the higher-order theories and it is difficult to formulate simple displacement-based C^0 elements satisfying both the surface traction conditions and the interlayer continuous conditions (Reddy 1984, Ren & Hinton 1986, Pandya and Kant 1988, Kapania & Raciti 1989, Cho and Parmerter 1994). By using a mixed formulation, Putcha and Reddy (1986) developed a C^0 plate element based on Reddy's third-order shear deformation theory (SHSDT) (Reddy 1984) in which eleven degrees of freedom are used at each node. This mixed finite element gives good results, but it is not efficient computationally. Pandya and Kant (1988) and Kant and Kommineni (1994) developed C^0 composite plate elements based on the higher-order shear deformation theory (HSDT) developed by Kant, Owen and Zienkiewicz (1982). The boundary conditions of the transverse shear stresses on the plate surfaces are neglected in the theory of Kant *et al.* (1982). And it is just the negligence of the traction free condition made it possible that Kant's HSDT plate elements (Pandya and Kant 1988, and Kant and Kommineni 1994) could be C^0-continuity. Furthermore, the numerical integration was used in these C^0 plate elements. Cho and Parmerter (1996) developed a C^0 triangular bending element based on an efficient higher order plate theory (EHOPT) (Cho and Parmerter 1992). However, this C^0 triangular bending element is valid for symmetric laminated plates only. The development of accurate and efficient composite plate elements is still receiving intensive attention from researchers (see, Reddy 1997). The zig-zag theory (Murakami 1986) has some attractive features, for example, the shear stress continuity at the layer interfaces is satisfied and the stress distribution across the plate thickness is accurate (Cho and Parmerter 1992 and 1994, Carrera 1996 and 1997 among others). But once again the numerical integration has to be employed in the composite plate elements based on the zig-zag theory (Cho and Parmerter 1994, Carrera 1996).

The objective of this paper is to present a simple quadrilateral C^0 composite plate element. This new C^0 composite plate element is formulated by using the Reddy-Levinson's simple third-order shear deformation theory (STSDT) (Reddy 1984, Levinson 1980), the assumed strain formulation (Tang, Chen and Liu 1980) and interrelated edge displacement and rotations along element boundaries (Hu 1981, Shi and Voyiadjis 1991). A special feature of the present composite plate element is that the element stiffness matrix is evaluated explicitly. The explicit stiffness matrix leads to high computational efficiency in the bending analysis of thick laminated composite plates, particularly in the nonlinear analysis where the element stiffness matrices have to be evaluated numerous times.

2. Displacement and strain fields

The displacement field in the Reddy-Levinson third-order shear deformation theory (Reddy 1984, Levinson 1980) can be written as

$$u(x,y,z)=u_0(x,y)-\phi_x(x,y)\,z-\frac{4}{3h^2}\left(\frac{\partial w_0}{\partial x}-\phi_x\right)z^3 \tag{1}$$

$$v(x,y,z)=v_0(x,y)-\phi_y(x,y)\,z-\frac{4}{3h^2}\left(\frac{\partial w_0}{\partial y}-\phi_y\right)z^3 \tag{2}$$

$$w(x,y,z)=w_0(x,y) \tag{3}$$

where u_0, v_0 and w_0 are the displacements of a point on the plate reference plane in the x-, y-, and z- directions respectively; ϕ_x and ϕ_y are the rotations of a normal to the reference plane about the y- and x- axes; and h is the total thickness of the plate. Let the first-order shear strains, which are the shear strains at $z=0$, be

$$\gamma_x=\frac{\partial w_0}{\partial x}-\phi_x \tag{4}$$

$$\gamma_y=\frac{\partial w_0}{\partial y}-\phi_y \tag{5}$$

Then Eqs. (1) and (2) take the form

$$u(x,y,z)=u_0(x,y)-\phi_x(x,y)z-\frac{4}{3h^2}\gamma_x z^3 \tag{6}$$

$$v(x,y,z)=v_0(x,y)-\phi_y(x,y)z-\frac{4}{3h^2}\gamma_y z^3 \tag{7}$$

Eqs. (6), (7) and (3) lead to the strains

$$e_x=\frac{\partial u_0}{\partial x}-\frac{\partial \phi_x}{\partial x}z-\frac{4}{3h^2}\frac{\partial \gamma_x}{\partial x}z^3 \tag{8}$$

$$e_y=\frac{\partial v_0}{\partial y}-\frac{\partial \phi_y}{\partial y}z-\frac{4}{3h^2}\frac{\partial \gamma_y}{\partial y}z^3 \tag{9}$$

$$e_{xy}=\frac{1}{2}\left[\frac{\partial u_0}{\partial y}+\frac{\partial v_0}{\partial x}-\left(\frac{\partial \phi_x}{\partial y}+\frac{\partial \phi_y}{\partial x}\right)z-\frac{4}{3h^2}\left(\frac{\partial \gamma_x}{\partial y}+\frac{\partial \gamma_y}{\partial x}\right)z^3\right] \tag{10}$$

$$e_{yz}=\frac{1}{2}\left(1-\frac{4}{h^2}z^2\right)\left(\frac{\partial w_0}{\partial y}-\phi_y\right) \tag{11}$$

$$e_{xz}=\frac{1}{2}\left(1-\frac{4}{h^2}z^2\right)\left(\frac{\partial w_0}{\partial x}-\phi_x\right) \tag{12}$$

$$e_z=0 \tag{13}$$

The in-plane strain vector $\boldsymbol{e}_p$ and transverse shear strain vector $\boldsymbol{e}_t$ can be written in terms of membrane strains $\boldsymbol{e}_m$, bending strains $\boldsymbol{e}_b$, transverse shear strains $\boldsymbol{e}_s$ and higher-order shear strains $\boldsymbol{e}_{hs}$ as

$$\boldsymbol{e}_p = \begin{Bmatrix} e_x \\ e_y \\ 2e_{xy} \end{Bmatrix} = \boldsymbol{e}_m^0 - \boldsymbol{e}_b z - \frac{4}{3h^2}\boldsymbol{e}_{hs} z^3 \tag{14}$$

$$\boldsymbol{e}_t = \begin{Bmatrix} 2e_{yz} \\ 2e_{xz} \end{Bmatrix} = \left(1 - \frac{4}{h^2} z^2\right)\boldsymbol{e}_s \tag{15}$$

with

$$\boldsymbol{e}_m = \begin{Bmatrix} e_x{}^0 \\ e_y{}^0 \\ 2e_{xy}^0 \end{Bmatrix} = \begin{Bmatrix} \dfrac{\partial u_0}{\partial x} \\ \dfrac{\partial v_0}{\partial x} \\ \dfrac{\partial u_0}{\partial y} + \dfrac{\partial v_0}{\partial x} \end{Bmatrix} \tag{16}$$

$$\boldsymbol{e}_b = \begin{Bmatrix} \kappa_x \\ \kappa_y \\ 2\kappa_{xy} \end{Bmatrix} = \begin{Bmatrix} \dfrac{\partial \phi_x}{\partial x} \\ \dfrac{\partial \phi_y}{\partial x} \\ \dfrac{\partial \phi_x}{\partial y} + \dfrac{\partial \phi_y}{\partial x} \end{Bmatrix} \tag{17}$$

$$\boldsymbol{e}_s = \begin{Bmatrix} \dfrac{\partial w_0}{\partial y} - \phi_y \\ \dfrac{\partial w_0}{\partial x} - \phi_x \end{Bmatrix} \tag{18}$$

$$\boldsymbol{e}_{hs} = \begin{Bmatrix} \dfrac{\partial \gamma_x}{\partial x} \\ \dfrac{\partial \gamma_y}{\partial x} \\ \dfrac{\partial \gamma_x}{\partial y} + \dfrac{\partial \gamma_y}{\partial x} \end{Bmatrix} \tag{19}$$

3. Strain energy density

The strain energy functional is used in the assumed strain element formulation. The equilibrium equations in terms of stress resultants and stress couples in the third-order shear deformation plate theory are different from those of the first-order shear plate theory (Reddy 1984). The variationally consistent equilibrium equations of the third-order plate theory can be derived using the principles of virtual work (Reddy 1997).

When the transverse shear stresses are accounted for, but the transverse normal stress is neglected, the strain energy density of a plate, U, is of the form

$$U = \frac{1}{2}\int_{-h/2}^{h/2} (\sigma_x e_x + \sigma_y e_y + 2\sigma_{xy} e_{xy} + 2\sigma_{yz} e_{yz} + 2\sigma_{xz} e_{xz})\, dz \tag{20}$$

For a laminated composite plate, the in-plane stresses, σ_p, and transverse shear stresses, σ_t, can be expressed in terms of strains as

$$\sigma_p = \begin{Bmatrix} \sigma_x \\ \sigma_y \\ \sigma_{xy} \end{Bmatrix} = \begin{bmatrix} Q_{11} & Q_{12} & Q_{16} \\ Q_{21} & Q_{22} & Q_{26} \\ Q_{61} & Q_{62} & Q_{66} \end{bmatrix} \begin{Bmatrix} e_x \\ e_y \\ 2e_{xy} \end{Bmatrix} = Q_p e_p \tag{21}$$

$$\sigma_t = \begin{Bmatrix} \sigma_{yz} \\ \sigma_{xz} \end{Bmatrix} = \begin{bmatrix} Q_{44} & Q_{45} \\ Q_{54} & Q_{55} \end{bmatrix} \begin{Bmatrix} 2e_{yz} \\ 2e_{xz} \end{Bmatrix} = Q_t e_t \tag{22}$$

in which $\boldsymbol{Q}_p$ and $\boldsymbol{Q}_t$ are, respectively, the transformed in-plane and out of plane elastic constant matrices in the plate coordinates (Reddy 1997). Substituting Eqs. (21), (22), (14) and (15) into Eq. (20) leads to

$$U = \frac{1}{2}\int_{-h/2}^{h/2} \left[\{e_m - e_b z - c e_{hs} z^3\}^T Q_p \{e_m - e_b z - c e_{hs} z^3\} + (1 - 3cz^2)^2 e_s^T Q_t e_s \right] dz \tag{23}$$

where $c = 4/(3h^2)$. By defining the generalized rigidity matrices

$$(A, B, D, E, F, H) = \int_{-h/2}^{h/2} (1, z, z^2, z^3, z^4, z^6) Q_p\, dz \tag{24}$$

$$S = \int_{-h/2}^{h/2} (1 - 6cz^2 + 9c^2 z^4)\, Q_t\, dz \tag{25}$$

Eq. (23) for U can be expressed as

$$\begin{aligned} U = \frac{1}{2}[&e_m^T A e_m + e_b^T D e_b + e_s^T S e_s + e_{hs}^T c^2 H e_{hs} \\ &- (e_m^T B e_b + e_b^T B e_m) - (e_m^T c E e_{hs} + e_{hs}^T c E e_m) + (e_b^T c F e_{hs} + e_{hs}^T c F e_b)] \end{aligned} \tag{26}$$

It should be noted that there are two more coupling terms in the above strain energy expression resulting from the third-order shear deformation theory. Unlike the stretching-bending coupling matrix $\boldsymbol{B}$, which vanishes in symmetric laminates, coupling matrix $\boldsymbol{F}$ is nonzero even in the case of symmetric laminates.

For the prescribed force boundary conditions, we define the stress resultants and stress couples

$$(\boldsymbol{N}, \boldsymbol{M}, \boldsymbol{P}) = \int_{-h/2}^{h/2} \sigma_p (1, z, z^3)\, dz \tag{27}$$

$$\boldsymbol{Q} = \int_{-h/2}^{h/2} (1 - 3cz^2)\, \sigma_t\, dz \tag{28}$$

where $\boldsymbol{P}$ is the vector of higher-order stress couples. It should be pointed out that transverse shear forces defined above are different from those used in the classical plate theory and in the first-order shear plate theories.

By using the principle of virtual displacements, it can be shown that the displacements of the third-order shear deformation theory in Eqs. (1) and (2) results in one additional boundary condition involving

$$\frac{\partial w}{\partial n} \quad \text{or} \quad P_n \tag{29}$$

in addition to the five boundary conditions of the first-order shear deformation theory, when the modified stress results and stress couples are used for the force boundary conditions in the third-order shear theory (Reddy 1984). In the above equation n signifies the in-plane normal direction of a plate boundary.

4. Finite element modeling

In finite element modeling, element strains in Eqs. (16)-(19) can, in general, be expressed in terms of the element nodal displacement vector $\boldsymbol{q}$ and element strain matrices as follows

$$\boldsymbol{e}_m = \boldsymbol{B}_m \boldsymbol{q}, \quad \boldsymbol{e}_b = \boldsymbol{B}_b \boldsymbol{q}, \quad \boldsymbol{e}_s = \boldsymbol{B}_s \boldsymbol{q}, \quad \boldsymbol{e}_{hs} = \boldsymbol{B}_{hs} \boldsymbol{q} \tag{30}$$

Consequently, the strain energy in an element of domain Ω, Π_e, takes the form

$$\begin{aligned} \Pi_e = \frac{1}{2} \boldsymbol{q}^T \int_\Omega [&\boldsymbol{B}_b^T \boldsymbol{D} \boldsymbol{B}_b + \boldsymbol{B}_m^T \boldsymbol{A} \boldsymbol{B}_m + \boldsymbol{B}_s^T \boldsymbol{S} \boldsymbol{B}_s + \boldsymbol{B}_{hs}^T c^2 \boldsymbol{H} \boldsymbol{B}_{hs} \\ &- (\boldsymbol{B}_m^T \boldsymbol{B} \boldsymbol{B}_b + \boldsymbol{B}_b^T \boldsymbol{B} \boldsymbol{B}_m) - (\boldsymbol{B}_m^T c \boldsymbol{E} \boldsymbol{B}_{hs} + \boldsymbol{B}_{hs}^T c \boldsymbol{E} \boldsymbol{B}_m) + (\boldsymbol{B}_b^T c \boldsymbol{F} \boldsymbol{B}_{hs} + \boldsymbol{B}_{hs}^T c \boldsymbol{F} \boldsymbol{B}_b)] d\Omega\, \boldsymbol{q} \end{aligned} \tag{31}$$

If we define the element bending, membrane, shear, higher-order shear and coupling stiffness matrices, respectively, as

$$\boldsymbol{K}_b = \int_\Omega \boldsymbol{B}_b^T \boldsymbol{D} \boldsymbol{B}_b\, d\Omega \tag{32}$$

$$\boldsymbol{K}_m = \int_\Omega \boldsymbol{B}_m^T \boldsymbol{A} \boldsymbol{B}_m\, d\Omega \tag{33}$$

$$\boldsymbol{K}_s = \int_\Omega \boldsymbol{B}_s^T \boldsymbol{S} \boldsymbol{B}_s\, d\Omega \tag{34}$$

$$\boldsymbol{K}_{hs} = \int_\Omega \boldsymbol{B}_{hs}^T c^2 \boldsymbol{H} \boldsymbol{B}_{hs}\, d\Omega \tag{35}$$

$$\boldsymbol{K}_c = \int_\Omega [-(\boldsymbol{B}_m^T \boldsymbol{B} \boldsymbol{B}_b + \boldsymbol{B}_b^T \boldsymbol{B} \boldsymbol{B}_m) - (\boldsymbol{B}_m^T c \boldsymbol{E} \boldsymbol{B}_{hs} + \boldsymbol{B}_{hs}^T c \boldsymbol{E} \boldsymbol{B}_m) + (\boldsymbol{B}_b^T c \boldsymbol{F} \boldsymbol{B}_{hs} + \boldsymbol{B}_{hs}^T c \boldsymbol{F} \boldsymbol{B}_b)] d\Omega \tag{36}$$

then Eqs. (31)-(36) lead to the element stiffness matrix $\boldsymbol{K}$ as

$$\boldsymbol{K} = \boldsymbol{K}_b + \boldsymbol{K}_m + \boldsymbol{K}_s + \boldsymbol{K}_{hs} + \boldsymbol{K}_c \tag{37}$$

The higher-order transverse shear stiffness matrix $\boldsymbol{K}_{hs}$ and the last two terms in the coupling matrix in Eq. (36) are the modification for the element stiffness matrix given by the first-order shear deformation theory.

5. Four-noded quadrilateral assumed strain element

5.1. Quasi-conforming element formulation

The element strain matrices in Eq. (30) can be evaluated simply and efficiently by the quasi-conforming element technique (Tang, Chen and Liu 1980), an assumed strain method. In the quasi-conforming elements, the element strain fields are interpolated directly over the element domain rather than derived from the assumed displacement fields, and the compatibility in an element domain is satisfied in a weak form. Let a *prime* signify the assumed strain field, when the continuity along inter-element boundaries is satisfied *a priori*, the element strain energy in Eq. (31) is then modified as

$$\Pi_e^* = \Pi_e + \int_\Omega \widetilde{\boldsymbol{M}}^T (e_b - e_b')\, d\Omega + \int_\Omega \widetilde{\boldsymbol{N}}^T (e_m - e_m')\, d\Omega + \int_\Omega \widetilde{\boldsymbol{Q}}^T (e_s - e_s')\, d\Omega + \int_\Omega \widetilde{\boldsymbol{P}}^T (e_{hs} - e_{hs}')\, d\Omega \tag{38}$$

where, $\widetilde{\boldsymbol{M}}$, $\widetilde{\boldsymbol{N}}$, $\widetilde{\boldsymbol{Q}}$ and $\widetilde{\boldsymbol{P}}$ and are the test functions corresponding to their relevant strain vectors.

5.2. Four-noded quadrilateral plate element

The element shown in Fig. 1 has seven degrees of freedom at each node. A suitable assumed element strain field for this element is of the form

$$e_b = \begin{bmatrix} 1 & x & y & xy & 0 & 0 & 0 & 0 & 0 & 0 & 0 \\ 0 & 0 & 0 & 0 & 1 & x & y & xy & 0 & 0 & 0 \\ 0 & 0 & 0 & 0 & 0 & 0 & 0 & 0 & 1 & x & y \end{bmatrix} \begin{Bmatrix} \alpha_{b1} \\ \alpha_{b2} \\ \cdot \\ \cdot \\ \cdot \\ \alpha_{b11} \end{Bmatrix} = \boldsymbol{P}_b \alpha_b \tag{39}$$

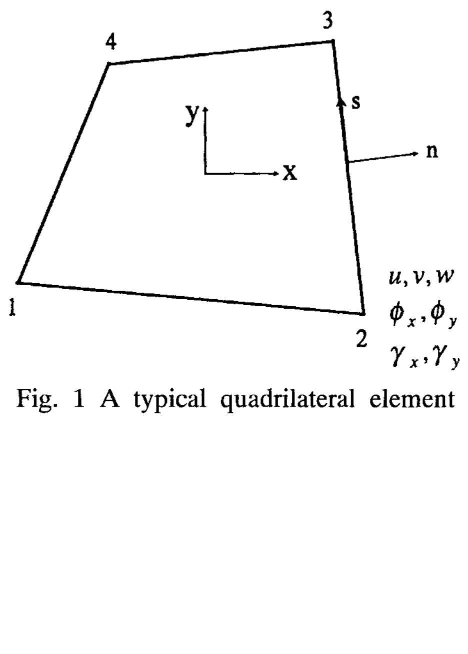

Fig. 1 A typical quadrilateral element

$$e_m = \begin{bmatrix} 1 & y & 0 & 0 & 0 \\ 0 & 0 & 1 & x & 0 \\ 0 & 0 & 0 & 0 & 1 \end{bmatrix} \begin{Bmatrix} \alpha_{m1} \\ \alpha_{m2} \\ \alpha_{m3} \\ \alpha_{m4} \\ \alpha_{m5} \end{Bmatrix} = P_m \alpha_m \tag{40}$$

$$e_s = \begin{bmatrix} 1 & 0 \\ 0 & 1 \end{bmatrix} \begin{Bmatrix} \alpha_{s1} \\ \alpha_{s2} \end{Bmatrix} = P_s \alpha_s \tag{41}$$

$$e_{hs} = \begin{bmatrix} 1 & y & 0 & 0 & 0 \\ 0 & 0 & 1 & x & 0 \\ 0 & 0 & 0 & 0 & 1 \end{bmatrix} \begin{Bmatrix} \alpha_{hs1} \\ \alpha_{hs2} \\ \alpha_{hs3} \\ \alpha_{hs4} \\ \alpha_{hs5} \end{Bmatrix} = P_{hs} \alpha_{hs} \tag{42}$$

where P_i and α_i ($i = b, m, s, hs$) are the strain interpolation matrices and strain parameters. It can be shown that the above assumed strain field satisfies the rank requirement for the element stiffness matrix. It is worthwhile to point out that the linear terms in the higher-order shear strains e_{hs} are merely to satisfy the rank requirement.

Let the weak forms of the compatibility in Eq. (38) be satisfied individually at the element level and the same interpolation functions be used for the test functions. Then we have

$$\int_\Omega P_i^T P_i \alpha_i \, d\Omega = \int_\Omega P_i^T e_i \, d\Omega, \quad i = b, m, s, hs \tag{43}$$

Consequently, the strain parameters can be evaluated in terms of element nodal displacement vector q as (Tang, Chen and Liu 1980, Shi and Voyiadjis 1991)

$$\alpha_i = A_i^{-1} C_i q, \quad i = b, m, s, hs \tag{44}$$

with

$$A_i = \int_\Omega P_i^T P_i \, d\Omega, \quad C_i q = \int_\Omega P_i^T e_i \, d\Omega, \quad i = b, m, s, hs \tag{45}$$

For the four-noded element shown in Fig. 1, the element nodal displacement vector q is of the form

$$q = \{q_1 \; q_2 \; q_3 \; q_4\}^T \tag{46}$$

$$q_j = \{u_j \; v_j \; w_j \; \phi_{xj} \; \phi_{yj} \; \gamma_{xj} \; \gamma_{yj}\}, \quad j = 1, 2, 3, 4 \tag{47}$$

Therefore, the strain matrices take the form

$$B_i = P_i A_i^{-1} C_i, \quad i = b, m, s, hs \tag{48}$$

A substitution of the strain matrices defined above into Eqs. (32) to (36) gives the element stiffness matrices. For example, $\boldsymbol{K}_{hs}$ is of the form

$$\boldsymbol{K}_{hs} = \boldsymbol{C}_{hs}^T \boldsymbol{A}_{hs}^{-T} \int_{\Omega} \boldsymbol{P}_{hs}^T c^2 \boldsymbol{H}\, \boldsymbol{P}_{hs}\, d\Omega\, \boldsymbol{A}_{hs}^{-1} \boldsymbol{C}_{hs} \tag{49}$$

The matrix $\boldsymbol{A}_i$ simply involves the integration of polynomials and can be evaluated easily (Shi and Voyiadjis 1991). Matrix $\boldsymbol{C}_i$ can be evaluated using integration by parts. For example

$$\boldsymbol{C}_{hs}\boldsymbol{q} = \int_{\Omega} \boldsymbol{P}_{hs}^T \begin{Bmatrix} \dfrac{\partial \gamma_x}{\partial x} \\ \dfrac{\partial \gamma_y}{\partial y} \\ \dfrac{\partial \gamma_x}{\partial y} + \dfrac{\partial \gamma_y}{\partial x} \end{Bmatrix} d\Omega = \int_{\Omega} \begin{Bmatrix} \dfrac{\partial \gamma_x}{\partial x} \\ y\dfrac{\partial \gamma_x}{\partial x} \\ \dfrac{\partial \gamma_y}{\partial y} \\ x\dfrac{\partial \gamma_y}{\partial y} \\ \dfrac{\partial \gamma_x}{\partial y} + \dfrac{\partial \gamma_y}{\partial x} \end{Bmatrix} d\Omega = \oint_{\partial\Omega} \begin{Bmatrix} \gamma_x n_x \\ y\ \gamma_x n_x \\ \gamma_y n_y \\ x\ \gamma_y n_y \\ \gamma_x n_y + \gamma_y n_x \end{Bmatrix} ds \tag{50}$$

where $\partial\Omega$ denotes the element boundary, ds is for the line integral, n_x and n_y are the direction cosines of an element boundary. By interpolating displacements in terms of the nodal variables along element boundary, the line integrals in the equation above can be carried out explicitly; $\boldsymbol{C}_b$, $\boldsymbol{C}_s$ and $\boldsymbol{C}_m$ can be evaluated in the same manner. The interrelated interpolations for edge displacement w_0 and tangential rotation ϕ_s (Hu 1981), in which w_0 is cubic and ϕ_s is quadratic, are employed in the evaluation of $\boldsymbol{C}_b$ and $\boldsymbol{C}_s$ to improve the accuracy and to satisfy the Kirchhoff assumption in thin plate analysis (Shi and Voyiadjis 1991).

Matrices $\boldsymbol{A}_i$ and $\boldsymbol{C}_i$ ($i = b, m, s, hs$) Eq. (46) are constant. The polynomial integrals appearing in Eq. (49) can be evaluated without numerical integration. Therefore, the element stiffness matrix proposed in this work can be evaluated explicitly, which leads to high computational efficiency.

Similar to the element QCCP-2 presented by Shi and Voyiadjis (1991), the present four-noded quadrilateral composite plate element can also be automatically reduced to the corresponding three-noded triangular element simply by making two adjacent nodes coincidence. However, the assumed displacement quadrilateral elements are not able to achieve this reduction (Zienkiewicz *et al.* 1993, Taylor and Auricchio 1993).

6. Numerical examples

The performance of a similar assumed strain plate element based on the first-order shear deformation theory was reported in the paper of Shi and Voyiadjis (1991). The efficiency and accuracy of the present higher-order strain element for the analysis of laminated composite plates are demonstrated in this section.

Example 1. Simply supported three-ply [0/90/0] square and rectangular plates

The three laminae of the composite plate have an equal thickness and same material properties. The material properties of the lamina are

$$E_1/E_2 = 25,\ G_{12}/E_2 = 0.5,\ G_{23}/E_2 = 0.2,\ \nu_{12} = 0.25.$$

In addition $G_{12} = G_{13}$. It should be noted that the lamina considered here is not transversely isotropic. The central deflections of the plate with aspect ratio $a/h = 10$ under a uniform load are solved to study the convergence of the present element. Only a quarter of the plate is considered because of the symmetry. Both regular and irregular meshes are considered. The irregular 2×2 and 4×4 mesh are shown in Fig. 2. The convergence curves are depicted in Fig. 3, in which w_{fem} represents the finite element solutions; w_{anal} signifies the analytical solutions given by Reddy's third-order shear deformation theory (Reddy 1984); and the number of elements per edge in Fig. 3 refers to a quarter of the plate. Let a be the dimension of the plate, q_0 be the density of the uniform load, the non-dimensional deflection can be defined as

$$\bar{w} = 100 \times w(0,0,0)\, E_2 h^3/(q_0 a^4)$$

The nondimensional analytical solution of Reddy's third-order theory is 1.09. It should be noted that finite element solutions depend also on the equivalent nodal loads. This is the reason that the deflection given by the particular irregular 2×2 mesh used here is better than that given by the regular 2×2 mesh. In general, regular meshes give better solutions than irregular meshes.

The deflections of square and rectangular composite plates under sinusoidal distributed load are also considered. The sinusoidal load is of the form

$$q(x,y) = q_0 \cos\frac{\pi x}{a} \cos\frac{\pi y}{b},\quad -\frac{a}{2} \le x \le \frac{a}{2},\quad -\frac{b}{2} \le y \le \frac{b}{2}$$

where a and b are, respectively, the dimensions of the plate in the x- and y-directions, and the coordinate origin is located at the plate center. The present non-dimensional central deflections of the square laminates under a sinusoidal distributed load are tabulated in Table 1, and those of the rectangular plates with $b = 3a$ are given in Table 2. The numerical results here are obtained from a 4×4 mesh for a quarter of the plate. ELS in Tables 1 and 2 represents the 3-D elasticity solutions of Pagano (1970). The HSDT solution of Pandya and Kant (1988) in Table 1 was obtained from a 2×2 mesh of nine-noded quadrilateral element. The EHOPT solutions in Table 2 were given by a 10×10 mesh of three-noded triangular element (Cho and Parmerter 1994). Table 1 also shows the influence of the shear correction factors, k, used in the first-order shear deformation theory on the deflections. The results in Table 1 and Table 2 show that the present element gives reasonable

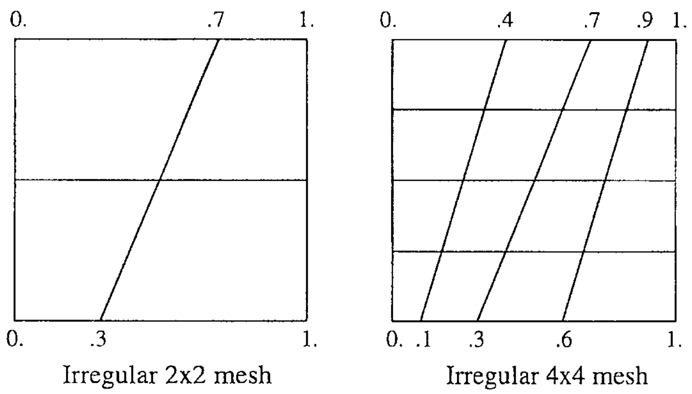

Fig. 2 Irregular 2×2 and 4×4 meshes

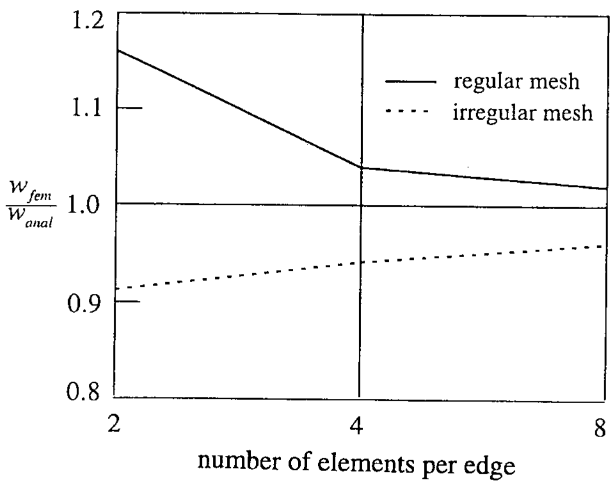

Fig. 3 Central deflections of a s.s. square laminate with $a/h=10$

Table 1 Non-dimensional central deflections of three-ply [0/90/0] square laminates under sinusoidal distributed load

a/h	Present	ELS (Pagano 1970)	STSDT (Reddy 1984)	HSDT (Pandya & Kant 1988)	FSDT (k=5/6) (Reddy 1984)	FSDT (k=1) (Reddy 1984)
4	1.945	2.002	1.922	-	1.776	1.568
10	0.711	0.715	0.713	0.716	0.670	0.631
100	0.431	0.433	0.434	-	0.434	0.433

Table 2 Non-dimensionalized deflections in three-ply [0/90/0] rectangular (b=3a) laminates under sinusoidal distributed load

a/h	Present	ELS (Pagano 1970)	STSDT (Reddy 1984)	EHOPT (Cho & Parmerter 1994)	FSDT (Reddy 1984)	CPT (Reddy 1984)
4	2.792	2.820	2.641	2.750	2.363	0.503
10	0.911	0.919	0.862	0.918	0.803	0.503
100	0.504	0.508	0.507	0.503	0.506	0.503

good results for very thick plates with $a/h=4$ and gives good solution for thin plates. The results in the tables also indicate that the higher-order shear deformation theories should be used in the analysis of laminated plates with aspect ratio $a/h\leq 10$ where the first-order theory gives significant errors.

Example 2. Simply supported four-ply [0/90/90/0] square plate subjected to a sinusoidal distributed load

This laminated composite plate consists of the same laminae with an equal ply thickness. The plate was studied analytically by Pagano and Hatfield (1972). The material properties of the lamina are the same as those in the previous example. A 4×4 mesh is used for a quarter of the plate in the present study. The non-dimensionalized deflections and stresses of the square laminates for different aspect ratios are tabulated in Table 3. The factor for the non-dimensional deflection is the same as that in the previous example, and non-dimensional stresses are defined as

Table 3 Non-dimensionalized deflections and stresses in four-ply [0/90/90/0] square laminated plates under sinusoidal distributed load

a/h	source	$\bar{w}$	$\bar{\sigma}_x$	$\bar{\sigma}_y$	$\bar{\sigma}_{xy}$	$\bar{\sigma}_{yz}$	$\bar{\sigma}_{xz}$
	Present	0.745	0.526	0.422	0.0297	0.169	0.265
	ELS (Pagano 1972)	0.737	0.559	0.401	0.0275	0.196	0.301
	Phan & Reddy (1985)	0.717	0.541	0.383	0.0265	0.153	0.263
10	Pandya & Kant (1988)	0.719	0.568	0.395	0.0273	0.172	0.270
	Argyris & Tenek (1993)	0.758	0.472	0.397	0.0249	0.207	0.298
	Cho & Parmerter (1994)	0.732	0.568	0.408	0.0272	0.146	0.309
	Carrera (RMZC) (1996)	0.752	0.586	0.422	0.0288	0.186	0.270
	Present	0.431	0.541	0.275	0.0193	0.149	0.296
	ELS (Pagano 1972)	0.434	0.539	0.271	0.0214	0.139	0.339
	Phan & Reddy (1985)	0.430	0.523	0.263	0.0208	0.103	0.280
100	Pandya & Kant (1988)	0.435	0.544	0.273	0.0215	0.124	0.301
	Argyris & Tenek (1993)	0.432	0.531	0.263	0.0208	0.147	0.328
	Cho & Parmerter (1994)	0.431	0.539	0.276	0.0216	0.141	0.337
	Carrera (RMZC) (1996)	0.435	0.565	0.284	0.0224	0.127	0.301

$$\bar{\sigma}_x = \sigma_x(0, 0, \frac{h}{2})h^2/(q_0a^2), \quad \bar{\sigma}_y = \sigma_y(0, 0, \frac{h}{4})h^2/(q_0a^2)$$

$$\bar{\sigma}_{xy} = -\sigma_{xy}(\frac{a}{2}, \frac{b}{2}, \frac{h}{2})h^2/(q_0a^2),$$

$$\bar{\sigma}_{yz} = \sigma_{zy}(0, \frac{b}{2}, 0)h/(q_0a), \quad \bar{\sigma}_{xz} = \sigma_{zx}(\frac{a}{2}, 0, 0)h/(q_0a)$$

The transverse shear stresses are evaluated from the equilibrium equations in which the derivatives of the bending strains are used. This shows the advantage of the linear bending strain field given in Eq. (39). Some analytical and numerical results are also given in the table for comparison. ELS in the table represents the 3-D elasticity solutions of Pagano and Hatfield (1972). A 8×8 mesh was used in the solutions of Argyris and Tenek (1993). The EHOPT results of Cho and Parmerter (1994) were given by a 10×10 mesh. The RMZC results of Carrera (1996) were given by a 2×2 mesh of Q9 element. The table shows that the present solutions agree well with the analytical and other numerical results. More examples on the accuracy of stresses and in-plane displacements across plate thickness given by the Reddy-Levinson third-order shear deformation theory can be found in Rohwer's paper (Rohwer 1991).

Example 3. Clamped and simply supported eight layer $[0/45/\text{-}45/90]_s$ square plates

The eight plies in the laminated plate have an equal thickness. The material properties of the plate are also the same as those in Example 1. Both simply supported and clamped boundary conditions are studied, and both uniform and sinusoidal distributed loads are considered. The non-dimensional central deflections are given in Table 4. However, Argyris and Tenek (1993) only gives the solutions of simply supported plates.

Example 4. Unsymmetric [0/90] cross-ply and antisymmetric [45/-45] angle-ply laminates

Both the cross-ply and the angle-ply laminates are square and simply supported, and all laminae

Table 4 Non-dimensionalized deflections in eight ply $[0/45/\text{-}45/90]_s$ square laminates under sinusoidal and uniform distributed loading

a/h	Source	Sinusoidal loading		Uniform loading	
		s.s.	clamped	s.s	clamped
4	Present	1.072	0.972	1.620	1.479
	Phan & Reddy (1985)	1.084	0.977	1.634	1.465
	Argyris & Tenek (1993)	1.094	-	1.631	-
10	Present	0.389	0.258	0.602	0.388
	Phan & Reddy (1985)	0.382	0.262	0.590	0.389
	Argyris & Tenek (1993)	0.380	-	0.588	-
100	Present	0.237	0.0705	0.375	0.0961
	Phan & Reddy (1985)	0.238	0.0699	0.377	0.0960
	Argyris & Tenek (1993)	0.238	-	0.380	-

have a same thickness. The material properties of the lamina of the cross-ply laminates are the same as those in Example 1, and the angle-ply lamina has the following properties:

$$E_1/E_2 = 40, \ G_{12}/E_2 = 0.6, \ G_{23}/E_2 = 0.5, \ \nu_{12} = 0.25$$

and $G_{12} = G_{13}$. Similar to that in Example 1, the lamina in this example is not transversely isotropic either. The non-dimensional central deflections of the laminates are given in Table 5. To study the influence of the stretching-bending coupling, both the results of the laminates with two layers (NL = 2) and the laminates with 10 layers (NL = 10) are given in the table. The laminates with aspect ratios of $a/h = 10$ and $a/h = 100$ are considered here, but only the results for $a/h = 10$ are available in Reddy's paper (1989).

7. Conclusions

Based on the Reddy-Levinson third-order plate theory, a four-noded quadrilateral C^0 plate element is presented in this paper for the bending analysis of thick laminated composite plates. The element has 7 degrees of freedom at each node. The element formulation is based on the assumed strain method, and the interrelated deflection and rotation interpolations along the element boundaries are employed. The resulting element does not need shear correction factors,

Table 5 Nondimensionalized deflections in cross-ply [0/90] and angle ply [45/-45] square laminates under uniform distributed load

NL	a/h	Cross-ply		Angle-ply	
		Present	Reddy (1989)	Present	Reddy (1989)
2	10	1.977	1.950	1.241	1.281
	100	1.643	-	0.623	-
10	10	0.965	0.958	0.691	0.632
	100	0.705	-	0.241	-

and the element stiffness matrix is evaluated explicitly. The present element with explicit element stiffness matrix can be coupled with the explicit time integration scheme for the dynamic problems, which will lead to a very computationally efficient finite element scheme in the dynamic analysis of thick laminated composite plates. The static analysis formulation presented in this work can easily be extended to dynamic analysis (Shi and Lam 1999).

References

Argyris, J. and Tenek, L. (1993), "A natural triangular layered element for bending analysis of isotropic, sandwich, laminated composite and hybrid plates", *Computer Meth. Appl. Mech. Eng.*, **109**, 197-218.

Carrera. E. (1996), "C^0 Reissner-Mindlin multilayered plate elements including zig-zag and interlaminar stress continuity", *Int. J. Num. Meth. Eng.*, **39**, 1797-1820.

Carrera. E. and Kroplin, B. (1997), "Zig-zag and interlaminar equilibria effects in large-deflection and postbuckling analysis of multilayered plates", *Mech. Comp. Mater. Struct.*, **4**, 69-94.

Cho, M. and Parmerter, R.R. (1992), "An efficient higher order plate theory for laminated plates", *Composite Structures,* **20**, 113-123.

Cho, M. and Parmerter, R. (1994), "Finite element for composite plate bending based on efficient higher order theory", *AIAA J.*, **32**, 2241-2248.

Hu, H.-C. (1981), *Variational Principles in Elasticity and Applications* (in Chinese), Science Press, Beijing.

Kant, T., Owen, D.R.J. and Zienkiewicz, O.C. (1982), "A refined higher-order C^0 plate bending element", *Comput. & Structures,* **15**, 177-183.

Kant, T. and Kommineni (1994), "Large amplitude free vibration analysis of cross-ply composite and sandwich laminates with a refined theory and C^0 finite elements", *Comput. & Structures,* **50**, 123-134.

Kapania, R.K. and Raciti, S. (1989), "Recent advances in analysis of laminated beams and plates, Part I: Shear effect and buckling", *AIAA J.,* **27**, 923-934.

Levinson, M. (1980), "An accurate, simple theory of the statics and dynamics of elastic plates", *Mech. Res. Commun.,* **7**, 343-350.

Murakami. H. (1986), "Laminated composite plate theory with improved in-plane responses", *J. Applied. Mech.,* **53**, 661-666.

Pagano, N.J. (1970), "Exact solutions for rectangular bidirectional composite anisotropic plates", *J. Comp. Materials,* **4**, 20-34.

Pagano, N.J. and Hatfield, S.J. (1972), "Elastic behavior of multilayered bidirectional composites", *AIAA J.,* **10**, 931-933.

Pandya, B.N. and Kant, T. (1988), "Flexural analysis of laminated composite using refined higher-order C^0 plate bending elements", *Computer Meth. Appl. Mech. Eng.,* **66**, 173-198.

Phan, N.D. and Reddy, J.N. (1985), "Analysis of laminated composite plates using a higher-order shear deformation theory", *Int. J. Num. Meth. Eng.,* **21**, 2201-2219.

Putcha, N.S. and Reddy, J.N., (1986), "Stability and natural vibration analysis of laminated plates by using a mixed element on a refined plate theory", *J. Sound Vib.,* **104**, 285-300.

Reddy, J.N. (1984), "A simple higher-order theory for laminated composites", *J. Applied. Mech.,* **51**, 745-752.

Reddy, J.N. (1989), "On refined computational models of composite laminates", *Int. J. Num. Meth. Eng.,* **27**, 361-382.

Reddy, J.N. (1997), *Mechanics of Laminated Composite Plates: Theory and Analysis,* CRC Press, Boca Raton, Florida.

Ren, J.G. and Hinton, E. (1986), "The finite element analysis of homogeneous and laminated composite plates using a simple higher-order theory", *Commun. Applied Num. Meth.,* **2**, 217-228.

Rohwer, K. (1991), "Application of higher order theories to the bending analysis of layered composite plates", *Int. J. Solids & Structures,* **29**, 105-119.

Shi, G. and Voyiadjis, G.Z. (1991), "Efficient and accurate four-noded quadrilateral C^0 plate element based on assumed strain fields", *Int. J. Num. Meth. Eng.,* **32**, 1041-1055.

Shi, G. and Lam K.Y. (1999), "Finite element vibration analysis of composite beams based on higher-order theory", *J. Sound and Vibration,* **219**, 707-721.

Tang, L., Chen, W. and Liu, Y. (1980), "The quasi-conforming element method and the generalized variational principle", *J. Dalian Inst. Tech.* (in Chinese), **19**, 1-15.

Taylor, L. and Auricchio, F. (1993), "Linked interpolation for Reissner-Mindlin plate elements, Part II: A simple triangle", *Int. J. Num. Meth. Eng.,* **36**, 3057-3066.

Zienkiewicz, O.C., Xu, Z., Zeng, L.F., Samuelsson, A. and Wiberg, N.E. (1993), "Linked interpolation for Reissner-Mindlin plate elements, Part I: A simple quadrilateral", *Int. J. Num. Meth. Eng.,* **36**, 3043-3056.